Journal of Affective Disorders 214 (2017) 53–59

Contents lists available at ScienceDirect

Journal of Affective Disorders

journal homepage: www.elsevier.com/locate/jad

Research paper

The left middle temporal gyrus in the middle of an impaired social-affective communication network in social anxiety disorder

Je-Yeon Yun[a,1], Jae-Chang Kim[b,1], Jeonghun Ku[c], Jung-Eun Shin[a], Jae-Jin Kim[d], Soo-Hee Choi[a,e,*]

[a] Department of Psychiatry, Seoul National University Hospital, Seoul, Republic of Korea
[b] Department of Nuclear Medicine, Yonsei University College of Medicine, Seoul, Republic of Korea
[c] Department of Biomedical Engineering, Keimyung University, Daegu, Republic of Korea
[d] Department of Psychiatry and Institute of Behavioral Science in Medicine, Yonsei University College of Medicine, Seoul, Republic of Korea
[e] Department of Psychiatry, Seoul National University College of Medicine and Institute of Human Behavioral Medicine, SNU-MRC, Seoul, Republic of Korea

ARTICLE INFO

Keywords:
Social anxiety disorder
Resting state functional connectivity
Graph theory
Left middle temporal gyrus
Intra-modular communication
Social-affective communication network

ABSTRACT

Background: Previous studies on patients diagnosed with social anxiety disorder (SAD) reported changed patterns of the resting-state functional connectivity network (rs-FCN) between the prefrontal cortices and other prefrontal, amygdalar or striatal regions. Using a graph theory approach, this study explored the modularity-based community profile and patterns of inter-/intra-modular communication for the rs-FCN in SAD.
Methods: In total, for 28 SAD patients and 27 healthy controls (HC), functional magnetic resonance imaging (fMRI) data were acquired in resting-state and subjected to a graph theory analysis.
Results: The within-module degree z-score for a hub region [out of a total of 10 hub regions ranked using the participation coefficient] named left middle temporal gyrus was impaired in SAD compared to HC, proportional to the severity of clinician-scored and patient-reported functional impairment in SAD.
Limitations: Most of participants included in this study were undergraduate students in their early-to-mid 20's.
Conclusions: This study showed the importance of functional communication from the left middle temporal gyrus with other opercular-insular-subcortical regions for better objective functioning and lesser subjective disability in SAD.

1. Introduction

Social anxiety disorder (SAD) is a common mental disorder with a point prevalence of 4.4% and lifetime prevalence of 6.1% (Ohayon and Schatzberg, 2010; Stein and Stein, 2008). Patients diagnosed with SAD suffer primarily from a notable fear and avoidance of most social or performance situations; repeated experiences of anxiety and fear against social threat such as scrutiny by others, even in seemingly harmless situations, interferes substantially with occupational performance as well as social relationship, and impairs quality of life in SAD (Stein and Kean, 2000; Stein and Stein, 2008). What is worse, typical compensatory maneuvers by SAD patients such as conducting attentive self-monitoring or repeating ruminative self-reflection on their own behavior often result in amplified perception of interpersonal stress and increased expression of negative emotions in response to stressful social events (Farmer and Kashdan, 2015; Hackmann et al., 2000). Furthermore, standard treatments for SAD using cognitive behavioral therapy (CBT) and pharmacotherapy improve clinical symptoms only to a moderate degree and a large proportion of SAD patients continue to suffer (Blanco et al., 2010; Davidson et al., 2004; Heimberg et al., 1998). Therefore, advanced treatment approaches based on a more integrated understanding of the neural underpinning of SAD symptomatology are in great need.

Prior studies of functional connectivity network in SAD have been focused on the imbalanced communication between the limbic region of the amygdala versus other cortical regions (Hattingh et al., 2012) during the emotional decoding of angry or contemptuous facial stimuli (Prater et al., 2013; Stein et al., 2002), classical conditioning for socially threatening stimuli (Pejic et al., 2013), and emotional regulation in preparation for public speech (Cremers et al., 2015). Moreover, inefficient prefrontal control of attentional focus by non-threatening distractor (Bishop, 2009) as well as insular hyper-activation toward

Abbreviations: HC, healthy controls; MTG, middle temporal gyrus; rs-FCN, resting state functional connectivity network; SAD, social anxiety disorder

* Correspondence to: Department of Psychiatry, Seoul National University Hospital, 101 Daehak-ro, Jongno-gu, Seoul 03080, Republic of Korea.
E-mail address: soohchoi@snu.ac.kr (S.-H. Choi).

[1] These authors contributed equally to this work.

http://dx.doi.org/10.1016/j.jad.2017.01.043
Received 25 September 2016; Received in revised form 27 December 2016; Accepted 23 January 2017
Available online 04 March 2017

inner-threatening cue [pulse-sound] in front of social situation [faces of crowd] (Choi et al., 2016) implied neural mechanism for the subjective misinterpretation of social situations in SAD underpinned the heightened awareness of fear-related interoceptive arousal and negative affective status despite effortful inner attempts at executive control (Diekhof et al., 2011; Yoon et al., 2016). However, a resting-state functional connectivity network (rs-FCN) approach, which reflects intrinsic functional brain organization in the lower-frequency [< 0.1 Hz] range during a task-free state (Biswal et al., 1995), demonstrated changed profile of functional crosstalk among broader brain regions in SAD (Fouche et al., 2013) encompassing the default mode network, salience and executive control networks, visual and sensorimotor networks, affective and reward networks (Liu et al., 2015b; Manning et al., 2015; Pannekoek et al., 2013; Peterson et al., 2014). Of note, altered strength of functional communication between the orbitofrontal cortex versus amygdala or executive control network components distinctively characterized SAD compared to HC (Geiger et al., 2016; Liu et al., 2015a). Furthermore, strength of the rs-FCN between amygdala and the anterior cingulate cortex was related to the intensity of social inhibition in general population (Blackford et al., 2014) as well as to the degree of symptom improvement in SAD after CBT or intranasal application of oxytocin (Dodhia et al., 2014; Klumpp et al., 2014; Whitfield-Gabrieli et al., 2015).

As a matter of fact, a recent pioneering study using the graph theory approach and modularity-based community detection successfully untangled the dynamic connectivity among cognitive and behavioral processes in SAD and demonstrated a primal role of orienting component of attention in the psychopathology of SAD by way of their influence toward the fear for and resultant avoidance of social situations (Heeren and McNally, 2016). However, there have been few studies on SAD to explore the graph theory-based global and regional rs-FCN network characteristics; the exact qualities of small-worldness reflecting the degree of balance between network integration [≈ lower average path length among the nodes in a network] versus functional segregation [≈ higher levels of triangular clustering constructed among the three neighboring nodes in a network] for rs-FCN network for SAD (Fornito et al., 2016) has not yet been clarified. Accordingly, this study aimed to explore the network characteristics of small-worldness and modularity-based community profile [in which each community was comprised of the non-overlapping groups of brain regions to maximize the number of within-group connection and minimizes the number of between-group connection in a network; a statistic term named modularity quantifies the degree to which a network could be subdivided into such clearly delineated communities] (Newman, 2006) for rs-FCN in SAD. In partcular, this study tried to elucidate a neural underpinning of functional impairment related to social anxiety symptoms in SAD, as reflected in the changed profile of inter- or intra-network functional communication between the hub brain regions versus other members of functional community.

2. Method

2.1. Participants

Using an internet-based advertisement targeting undergraduate students, we recruited a total of 28 patients diagnosed with SAD, and 27 HC who closely matched for age, sex, years of education with SAD. With clinical interview with a licensed psychiatrist, each participant was evaluated for diagnosis with SAD using DSM-IV-TR criteria [classified as SAD] or for confirmation of no prior history of/current morbidity with psychiatric disorders using DSM-IV-TR criteria [classified as HC]. Degree of psychopathology as well as for functional disability were also scored using various scales including the Liebowitz Social Anxiety Scale (LSAS) (Liebowitz, 1987), the Hamilton Anxiety Scale (HAM-A) (Bruss et al., 1994), and the Global Assessment of Functioning (GAF). In addition, a package of self-report questionnaires including the Social Interaction Anxiety Scale (SIAS), Social Phobia Scale (SPS), Brief Version of the Fear of Negative Evaluation Scale (B-FNE), Beck Depression Inventory (BDI), and Sheehan Disability Scale (SDS) were used to measure the degree of perceived anxiety for interpersonal interaction or social performance, degree of negative apprehension for negative evaluation from others, and severity of depressive symptomatology, and perceived severity of functional impairment in relation to the clinical symptoms of SAD, respectively (Beck et al., 1961; Leary, 1983; Mattick and Clarke, 1998; Park and Kim, 2010; Sheehan, 1983). No volunteer with a previous history or current diagnosis of a clinically meaningful medical or neurological diseases, years of education < 12 yrs, or a BDI total score ≥21 was included in this study (Hahn et al., 1986). This study was approved by the institutional review board of Gangnam Severance Hospital. Written informed consent was obtained from every participant after thorough information for this study was provided.

2.2. Functional magnetic resonance imaging (MRI) data acquisition and pre-processing

Using a whole-body 1.5-T MRI system (Signa Eclipse; GE Medical Systems, Milwaukee, WI, USA) with an echo-planar imaging sequence (64×64×30 matrix; TR/TE =2000/22 ms; FOV =240 mm; FA =90°), blood oxygen level-dependent (BOLD) signals during resting status functional MRI [rs-fMRI; participants were instructed to do nothing in particular and rest with both eyes closed] were acquired for a total of 5 min (a total of 150 slices) per participant. In addition, using the same MRI equipment, a high-resolution T1-weighted images using a fast spoiled gradient echo sequence (256×256×116 matrix; TR/TE =8.5/1.8 ms; FOV =240 mm; FA =12°) were also obtained.

We pre-processed the rs-fMRI data using Statistical Parametric Mapping 12 software (SPM12; http://www.fil.ion.ucl.ac.uk/spm/software/spm12/). After initial exclusion of the first five slices, the remaining rs-fMRI image slices were corrected for slice timing, co-registered to the reference slice, realigned to Montreal Neurological Institute (MNI) anatomical space using a six-parameter rigid body affine transformation, normalized for signal intensity, and finally smoothed using a Gaussian kernel with 8-mm full-width-at-half-maximum (FWHM). Finally, using an in-house script running by way of Matlab R2014b (www.mathworks.com/products/matlab/), these preprocessed rs-fMRI data were band-pass filtered in terms of the temporal dimension [0.009–0.08 Hz], regressed out for the effects of head motion as well as for the nuisance signals from brain white matter, cerebrospinal fluid and global brain signal (Shin et al., 2014). Finally, regional time-series of processed BOLD signal for a total of 90 cerebral regions-of-interest (ROIs) comprising the Automated Anatomic Labeling (AAL) atlas (Tzourio-Mazoyer et al., 2002) were extracted, to calculate the individual correlation matrix of resting state functional connectivity network consisting of Pearson's correlation coefficients [$r > 0$] between two different ROIs per participant.

2.3. Graph theory analyses

To examine the characteristics of rs-FCN for SADs and HCs in terms of small-world and modular organization, a total of five global network characteristics including (1) *gamma* [normalized characteristic path length; the number of processing steps between different brain regions along the routes of functional connectivity, normalized as a ratio to values calculated from 1000 randomly rewired null model] (Rubinov and Sporns, 2010; Maslov and Sneppen, 2002), (2) *lambda* [normalized clustering coefficient; the fraction of triangles comprised of the neighboring brain regions in local network, averaged across the whole brain and normalized as a ratio to values calculated from 1000 randomly rewired null model] (Watts and Strogatz, 1998; Maslov and Sneppen, 2002), (3) *sigma* (small-worldness = *gamma*/*lambda*), (4) *Eglob* [normalized global efficiency; the average of the inverse shortest

Table 1
Demographic and clinical characteristics of patients and controls.

Characteristics	Group; mean ± SD				
	SAD, n =28	Controls, n =27	Statistic	*Cohen's d*	p value
Age, yr	23.5 ± 2.5	24.2 ± 1.9	$t_{53} = -1.1$	−0.315	0.278
Sex, male: female	19:09	17:10	$\chi_1 = 0.1$	–	0.703
Education level, yr[b]	15.0 ± 1.5	14.4 ± 1.7	$t_{50} = 1.3$	0.374	0.186
Age of disease onset, yr	16.0 ± 3.9	–	–	–	–
Global assessment of functioning	70.0 ± 11.14	–	–	–	–
Sheehan Disability Scale[c]	11.5 ± 4.6	–	–	–	–
Liebowitz Social Anxiety Scale[d]	73.7 ± 12.5	14.1 ± 8.7	$t_{48} = 19.2$	5.534	< 0.001
Social interaction anxiety scale[d]	45.2 ± 11.8	9.2 ± 5.0	$t_{36.3} = 14.4$	3.973	< 0.001
Social phobia scale[d]	38.3 ± 14.8	3.3 ± 3.8	$t_{30.0} = 11.9$	3.239	< 0.001
Brief fear of negative evaluation scale[e]	44.6 ± 7.2	25.3 ± 6.3	$t_{50} = 10.3$	2.853	< 0.001
Hamilton Anxiety scale[b]	11.8 ± 9.6	1.0 ± 1.8	$t_{29.2} = 5.8$	1.564	< 0.001
Beck depression inventory[d]	12.0 ± 6.8	2.6 ± 3.2	$t_{38.1} = 6.4$	1.769	< 0.001

SAD = social anxiety disorder; SD = standard deviation.
[a]Data are given as mean ± standard deviation.
[b] Data missing for 3 controls.
[c] Data missing for 1 SAD.
[d] Data missing for 1 SAD and 4 controls.
[e] Data missing for 1 SAD and 2 controls.

path length, normalized as a ratio to values calculated from 1000 randomly rewired null model] (Latora and Marchiori, 2001; Fagiolo, 2007; Rubinov and Sporns, 2010; Maslov and Sneppen, 2002) and (5) Q [modularity; the degree to which a network could be decomposed into relatively clearly delineated communities, calculated using the heuristic 'modularity_und.m' function of the Brain Connectivity Toolbox and averaged over the 500 runs of calculation] (Newman, 2006; Rubinov and Sporns, 2010) were calculated for binarized rs-FCN per participant across broad-ranged connection density (sparsity) of K =0.05–0.30 (with 0.01 increment) (Uehara et al., 2014).

Subsequently, a specific non-random sparsity range of K =0.10–0.23 as defined using three constraints of (1) at least 99% of nodes are connected, (2) small-worldness ($\sigma > 1$), and (3) modularity (Q) > 0.3 (Uehara et al., 2014) was selected to compare the global network characteristics between SAD versus HC and to explore the modular composition of group-averaged and binarized rs-FCNs using Infomap algorithm (Rosvall and Bergstrom, 2008). Focusing on the specific sparsity range of K =0.10–0.14 along which pre-defined optimal five module structures were consistently observed, top ten-ranked brain regions in terms of participation coefficient calculated from the group [HC]-averaged and binarized [K =0.10–0.14] rs-FCN were defined as hub regions (Power et al., 2013). Finally, under the optimal five module structures (see above), degree of inter-modular communication [participation coefficient] as well as intra-modular communication [intra-module degree z-score] for these 10 hub regions were calculated per participant [binarized individual rs-FCN across K =0.10–0.14] and were compared between SAD and HC using independent t-tests ($P < 0.05$).

All of these graph theory analyses were conducted using the Brain Connectivity Toolbox (Rubinov and Sporns, 2010). Visualization of modular composition for rs-FCNs was performed using BrainNet Viewer version 1.53 (Xia et al., 2013). Plots to illustrate global network characteristics [with error bars], inter-group differences of intra-modular degree z-score in hub region(s) [barplot] as well as correlation between those hub characteristics and clinical variable(s) [scatterplot] were drawn using Matlab R2014b (http://kr.mathworks.com/products/matlab/).

2.4. Statistical analysis of demographic and clinical variables

Inter-group comparisons of demographic and clinical variables were conducted using independent t-tests (for continuous variables) or chi-square test (for categorical variables) ($p < 0.05$). Moreover, Pearson's correlation coefficients were calculated to measure degree of relationship between clinical variables versus *intra-module degree z-score* for the hub regions (please refer to the 'graph theory analyses' section above). Admitting the explorative nature of inter-group comparisons for inter-modular communication, we did not apply a statistical correction for multiple comparisons (i.e., $p < 0.05$, uncorrected). All of these inter-group comparisons were performed using statistical toolbox of Matlab R2014b (www.mathworks.com/products/matlab).

3. Results

3.1. Participants

Demographic and clinical characteristics of the study participants are described in Table 1. Data were analyzed from 28 patients with a diagnosis of SAD and 27 HCs who did not show statistically significant differences for age, sex, and years of education (all $p > 0.05$). All SADs were medication-naïve at the time of study participation, were right-handed, and demonstrated statistically significant differences in clinical symptomatology as measured using LSAS, SIAS, SPS, FNES, HAM-A and BDI compared to HCs (all $p < 0.001$).

3.2. Resting state functional connectivity network: global characteristics

Over the non-random connection density range of K=0.10–0.23, the binarized rs-FCN of HCs and patients diagnosed with SAD satisfied three constraints of: (1) at least 99% of nodes are connected, (2) small-worldness ($\sigma > 1$), and (3) modularity (Q) > 0.3 (Uehara et al., 2014) and demonstrated comparable (all $p > 0.05$) area under the curve (AUC) values for normalized clustering coefficient (gamma; T=−0.121, p=0.904), normalized characteristic path length (lambda; T=−1.190, p=0.240), small-worldness (sigma; T=0.589, p=0.558), normalized global efficiency (GE; T=1.013, p=0.316) and modularity (Q; T=−0.285, p=0.777) (Fig. 1).

3.3. Resting state functional connectivity network: module composition

Community detection using Infomap algorithm (Rosvall and Bergstrom, 2008) for group-averaged and binarized rs-FCN matrices

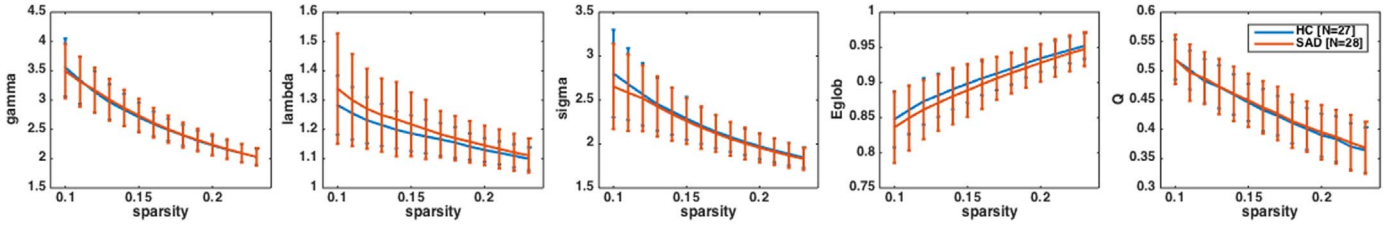

Fig. 1. Global characteristics of resting state functional connectivity in healthy controls (green) and social anxiety disorder (orange): (A) gamma (normalized clustering coefficient), (B) lambda (normalized characteristic path length), (C) sigma (small-worldness), (D) normalized global efficiency, and (E) modularity (Q). HC = healthy controls; SAD = social anxiety disorder.

of HCs identified a total of five modules across sparsity range of K =0.10–0.14. On the other hand, additional exploration of community structure for group-averaged and binarized rs-FCN in HC over the K ≥0.15 yielded less distinctive modular profile comprised of a total of three or four communities. Accordingly, the sparsity range of interest for community detection and subsequent calculation of participation coefficient as well as within-module degree z-score was confined across K =0.10–0.14; module 1 [fronto-parietal module] was comprised of the bilateral paracentral, superior and inferior parietal, superior and middle frontal, middle cingulate and supplementary motor cortices and precuneus. Module 2 [subcortical and fronto-temporal opercular module] encompassed bilateral insula, superior-middle temporal as well as inferior frontal cortices, and bilateral subcortical nuclei of thalamus, putamen and pallidum. Module 3 [prefrontal-caudate module] covered bilateral caudate as well as bilateral orbitofrontal, anterior cingulate, and superior medial frontal cortices. Module 4 [posterior parieto-occipital module] was comprised of posterior parietal regions of precuneus, posterior cingulate and angular cortices as well as occipital cortices. Finally, limbic regions including bilateral hippocampi and amygdalae surrounded by bilateral parahippocampal, inferior temporal and fusiform cortices constructed module 5 [limbic module] (Fig. 2).

3.4. Resting state functional connectivity network: Hub-related characteristics

Based on the rank of participation coefficient for all of the 90 nodes calculated from group-averaged and binarized rs-FCNs for HCs over the sparsity range of K=0.10–0.14, a total of 10 nodes [ranked as top 12%(=90×0.12≈10)] including bilateral middle temporal, right superior temporal and inferior frontal (pars triangularis) cortices [all module 2 members], left supramarginal right middle frontal gyri [all module 1 members], left angular and right lingual gyri [module 4 member], as well as right hippocampus and left inferior temporal gyrus [all module 5 members] were listed as hub regions; there was no statistically significant difference of participation coefficient for these ten brain regions between HCs versus SADs (all $p > 0.05$; independent t-tests).

On the contrary, within-module degree z-score calculated for these 10 hub regions demonstrated statistically significant ($p < 0.05$) attenuation of intra-modular functional communication during resting status in SAD between left middle temporal gyrus (MTG) versus other members of module 2 [subcortical and fronto-temporal opercular module] (T=2.25, p=0.029; independent t-test). Moreover, this value of within-module degree z-score for right middle temporal gyrus showed statistically significant correlations with both clinician-rated

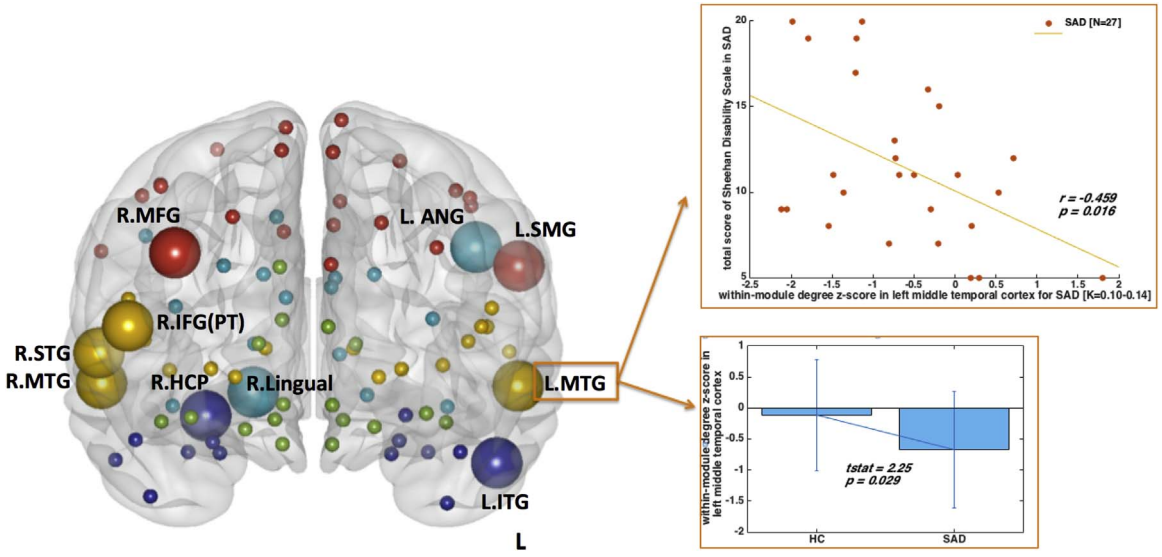

Fig. 2. Five modular composition of 90 AAL regions-of-interest (depicted with red, yellow, green, blue and purple, respectively) in group-averaged and binarized resting state functional connectivity network of healthy controls (HCs) across sparsity range of K =0.10–0.14. Specifically, a total of ten hubs [top 12%-ranked for participation coefficient] were demonstrated with bigger spheres and were marked with abbreviated names. Inter-group comparison of these ten hubs for participation coefficient did not revealed statistically significant differences between HCs and patients diagnosed with social anxiety disorder (SAD; all Ps > 0.05). On the other hand, intra-modular degree z-score [a composite score of intra-modular communication between specific node with other community members] for left middle temporal gyrus was attenuated in SAD compared to HC (boxplot in the lower right side; error-bars describe standard deviation per group). Furthermore, subjective degree of functional impairment as measured using total score of Sheehan disability score (SDS) showed statistically significant relationship with within-module degree z-score for left middle temporal gyrus in SAD (scatterplot in the upper right side). Abbreviation: L.ANG, left angular gyrus; L.ITG, left inferior temporal gyrus; L.MTG, left middle temporal gyrus; L.SMG, left supramarginal gyrus; R.HCP, right hippocampus, R.IFG(PT), right inferior frontal gyrus (pars triangularis); R.Lingual, right lingual gyrus; R.MFG, right middle frontal gyrus; R.MTG, right middle temporal gyrus; R.STG, right superior temporal gyrus.

(total score of GAF; r =0.421, p=0.026) and patient-reported (total score of SDS; r=−0.459, p=0.016) severity of functional impairment (Fig. 2). On the other hand, there was no statistically significant relationship between the BDI total score versus within-module degree z-score of the left middle temporal gyrus in this population (r=−0.030, p=0.837 when SAD and HC participants combined; r = 0.070, p= 0.731 for SAD only; r=−0.193, p=0.379 for HC only). This could provide evidence that the present findings (=inter-group difference of within-module degree z-score of the left middle temporal gyrus between SAD and HC) do not merely mirror difference in depressive symptoms as measured using BDI between the two groups.

4. Discussion

To the best of the authors' knowledge, this study is the first to explore the network characteristics of small-worldness and modularity-based community profile for rs-FCN in SAD. Specifically, in terms of global and regional network characteristics, using a graph theory approach, this study elucidated a neural underpinning of functional impairment related to the social anxiety symptoms in SAD. Global network characteristics including small-worldness (σ), global efficiency (GE) as well as modularity (Q) were comparable (all $p > 0.05$ for AUC across a sparsity range of K =0.10–0.23) between HCs and SADs. Furthermore, hub profile of rs-FCN in HC comprised of a total of 10 prefronto-parieto-temporal regions was also effective in SAD. On the other hand, the intra-modular degree z-score for a hub region [out of a total of 10 hub regions as ranked using participation coefficient] named left MTG was impaired in SAD compared to HC (T=2.25, p=0.029) proportional to the severity of objective (GAF) and subjective (SDS) functional impairment in SAD.

4.1. Changed structural and functional characteristics of left MTG in SAD

Compared to non-patient population, patients diagnosed with SAD showed changed characteristics of left MTG in terms of reduced gray matter density, decreased value of fractional anisotropy (FA), increased negative functional connectivity with amygdala, and attenuated amplitude of low-frequency fluctuations (ALFF) (Pannekoek et al., 2013; Qiu et al., 2014, 2015; Shang et al., 2014). However, albeit in the context of these changed structural and functional characteristics, the left MTG sustained the characteristics of being one of the network hubs [based on the degree-based centrality measure] in the scale-free network of resting state functional connectivity in SAD (Liu et al., 2015b), in concordance with the result of current study. Using participation coefficient, a measure of hubness optimized for correlation coefficient-based networks including resting state functional connectivity (Power et al., 2013), this study demonstrated the importance of left MTG as hub region that mediates functional crosstalk between different functional modules in the rs-FCN of SAD. Intuitively, we could presume lowered cognitive functioning, presence of clinical symptomatology or role-functioning (Kambeitz et al., 2016; van den Heuvel and Sporns, 2013; Warren et al., 2014) in SAD underpinned with 'microscopic brain lesion' of hub region such as left MTG (Pannekoek et al., 2013; Qiu et al., 2014, 2015; Shang et al., 2014), as reflected in the lowered within-module degree z-score of left MTG in this study.

4.2. Left MTG, in the middle of the social-affective communication network

This study demonstrated attenuated strength of intra-modular communication [measured using within-module degree z-score] between left MTG versus other community members of pars triangularis and opercularis, superior temporal cortices, bilateral insula and rolandic operculum as well as subcortical nuclei such as thalamus and putamen in SAD compared to HC. Left MTG comprises so-called speech network with language network components of inferior frontal and superior temporal cortices as well as with subcortical nuclei of thalamus and putamen (Tomasi and Volkow, 2012; Yu et al., 2011). In particular, when it comes to the communicative speech production using the second language [with limited capability of use as a communication tool], improved oral proficiency or lowered anxiety level for communicative speech using the second language were accompanied by increased BOLD signal changes of left MTG or left insula, respectively (Jeong et al., 2016). Moreover, reflecting the typical usage of language for communicative speech that involves goal-directed action targeted at another person in the context of social interaction, left MTG and the language network showed tight relationship with theory-of-mind functioning (Kandylaki et al., 2015); in functional communication with insula and thalamus as another network, the posterior components of speech network including superior temporal and MTG were involved with affective communication conveyed by empathic decoding of others' pain experience (Lang et al., 2011; Luo et al., 2014). Therefore, decreased intra-modular communication mediated by left MTG in the social-affective communication network could underlie faulty perception of emotional threat from others as well as less proficient use of language in SAD when exposed to social situations such as participating social communication or performing public speech, leading to the experience of severe distress and related functional impairment [measured using GAF or SDS] (Berthier et al., 2016; Choi et al., 2016; Cremers et al., 2015). In other words, attenuated strength of intra-modular communication between left MTG in the middle of social-affective communication network could be a neural correlate mediating the influence of heightened orienting attention for social interaction into the fear for and resultant avoidance of which in SAD (Heeren and McNally, 2016).

4.3. Limitations

This study has some limitations to be stated. Firstly, as most of participants included in this study were undergraduate students in their early-to-mid 20's, generalization of the study result toward SAD patients with broader range of age distribution could be limited. Secondly, focused exploration of changed network characteristics in hub-related fashion as well as usage of predefined brain parcellation using AAL90 atlas might inevitably affect the range of window to detect inter-group difference of rs-FCN profile in this study. However, independent component analysis-based network community detection might restrict further exploration for subcomponents (= specific brain regions of interest) of rs-FCN community; voxel-based network approaches such as global brain connectivity or functional connectivity density mapping are not suitable for detection of distinctive functional communities in the given rs-FCN.

5. Conclusions

In conclusion, this study revealed global and regional rs-FCN characteristics for SAD. With sustained network integrity in terms of small-worldness, modularity and global efficiency, patients diagnosed with SAD also shared comparable hub profile (calculated using the participation coefficient) with HC participants. When deeply inspected for intra-modular communication between hub regions versus other community members, left MTG comprising the social-affective communication network showed markedly reduced within-module degree z-score, in proportion to the severity of clinical symptom-related functional impairment of patients diagnosed with SAD; this hub-related imbalance of functional connectivity could possibly underlie frequent experience of severe distress in SAD when exposed to the public situations requiring social communication or social speech.

Acknowledgements

This study was funded by the Basic Science Research Program through the National Research Foundation of Korea (NRF) funded by the Ministry of Science, ICT & Future Planning (2014R1A1A1004553) and Aspiring Researcher Program through Seoul National University (SNU) in 2014.

References

Beck, A.T., Ward, C.H., Mendelson, M., Mock, J., Erbaugh, J., 1961. An inventory for measuring depression. Arch. Gen. Psychiatry 4, 561–571.
Berthier, M.L., Roe-Vellve, N., Moreno-Torres, I., Falcon, C., Thurnhofer-Hemsi, K., Paredes-Pacheco, J., Torres-Prioris, M.J., De-Torres, I., Alfaro, F., Gutierrez-Cardo, A.L., Baquero, M., Ruiz-Cruces, R., Davila, G., 2016. Mild developmental foreign accent syndrome and psychiatric comorbidity: altered white matter integrity in speech and emotion regulation networks. Front. Hum. Neurosci. 10, 399.
Bishop, S.J., 2009. Trait anxiety and impoverished prefrontal control of attention. Nat. Neurosci. 12, 92–98.
Biswal, B., Yetkin, F.Z., Haughton, V.M., Hyde, J.S., 1995. Functional connectivity in the motor cortex of resting human brain using echo-planar mri. Magn. Reson. Med 34, 537–541.
Blackford, J.U., Clauss, J.A., Avery, S.N., Cowan, R.L., Benningfield, M.M., VanDerKlok, R.M., 2014. Amygdala-cingulate intrinsic connectivity is associated with degree of social inhibition. Biol. Psychol. 99, 15–25.
Blanco, C., Heimberg, R.G., Schneier, F.R., Fresco, D.M., Chen, H., Turk, C.L., Vermes, D., Erwin, B.A., Schmidt, A.B., Juster, H.R., Campeas, R., Liebowitz, M.R., 2010. A placebo-controlled trial of phenelzine, cognitive behavioral group therapy, and their combination for social anxiety disorder. Arch. Gen. Psychiatry 67, 286–295.
Bruss, G.S., Gruenberg, A.M., Goldstein, R.D., Barber, J.P., 1994. Hamilton anxiety rating scale interview guide: joint interview and test-retest methods for interrater reliability. Psychiatry Res. 53, 191–202.
Choi, S.H., Shin, J.E., Ku, J., Kim, J.J., 2016. Looking at the self in front of others: neural correlates of attentional bias in social anxiety. J. Psychiatr. Res 75, 31–40.
Cremers, H.R., Veer, I.M., Spinhoven, P., Rombouts, S.A., Yarkoni, T., Wager, T.D., Roelofs, K., 2015. Altered cortical-amygdala coupling in social anxiety disorder during the anticipation of giving a public speech. Psychol. Med 45, 1521–1529.
Davidson, J.R., Foa, E.B., Huppert, J.D., Keefe, F.J., Franklin, M.E., Compton, J.S., Zhao, N., Connor, K.M., Lynch, T.R., Gadde, K.M., 2004. Fluoxetine, comprehensive cognitive behavioral therapy, and placebo in generalized social phobia. Arch. Gen. Psychiatry 61, 1005–1013.
Diekhof, E.K., Geier, K., Falkai, P., Gruber, O., 2011. Fear is only as deep as the mind allows: a coordinate-based meta-analysis of neuroimaging studies on the regulation of negative affect. Neuroimage 58, 275–285.
Dodhia, S., Hosanagar, A., Fitzgerald, D.A., Labuschagne, I., Wood, A.G., Nathan, P.J., Phan, K.L., 2014. Modulation of resting-state amygdala-frontal functional connectivity by oxytocin in generalized social anxiety disorder. Neuropsychopharmacology 39, 2061–2069.
Fagiolo, G., 2007. Clustering in complex directed networks. Phys. Rev. E. Stat. Nonlinear Soft Matter Phys. 76, 026107.
Farmer, A.S., Kashdan, T.B., 2015. Stress sensitivity and stress generation in social anxiety disorder: a temporal process approach. J. Abnorm. Psychol. 124, 102–114.
Fornito, A., Zalesky, A., Bullmore, E., 2016. Fundamentals of brain network analysis. Elsevier, London.
Fouche, J.P., van Der Wee, N.J., Roelofs, K., Stein, D.J., 2013. Recent advances in the brain imaging of social anxiety disorder. Hum. Psychopharmacol. 28, 102–105.
Geiger, M.J., Domschke, K., Ipser, J., Hattingh, C., Baldwin, D.S., Lochner, C., Stein, D.J., 2016. Altered executive control network resting-state connectivity in social anxiety disorder. World J. Biol. Psychiatry 17, 47–57.
Hackmann, A., Clark, D.M., McManus, F., 2000. Recurrent images and early memories in social phobia. Behav. Res. Ther. 38, 601–610.
Hahn, H.M., Yum, T.H., Shin, Y.W., Kim, T.H., Yoon, D.J., Chung, K.J., 1986. A standardization study of beck depression inventory in korea. J. Korean Neuropsychiatr. Assoc., 25.
Hattingh, C.J., Ipser, J., Tromp, S.A., Syal, S., Lochner, C., Brooks, S.J., Stein, D.J., 2012. Functional magnetic resonance imaging during emotion recognition in social anxiety disorder: an activation likelihood meta-analysis. Front. Hum. Neurosci. 6, 347.
Heeren, A., McNally, R.J., 2016. An integrative network approach to social anxiety disorder: the complex dynamic interplay among attentional bias for threat, attentional control, and symptoms. J. Anxiety Disord. 42, 95–104.
Heimberg, R.G., Liebowitz, M.R., Hope, D.A., Schneier, F.R., Holt, C.S., Welkowitz, L.A., Juster, H.R., Campeas, R., Bruch, M.A., Cloitre, M., Fallon, B., Klein, D.F., 1998. Cognitive behavioral group therapy vs phenelzine therapy for social phobia: 12-week outcome. Arch. Gen. Psychiatry 55, 1133–1141.
Jeong, H., Sugiura, M., Suzuki, W., Sassa, Y., Hashizume, H., Kawashima, R., 2016. Neural correlates of second-language communication and the effect of language anxiety. Neuropsychologia 84, e2–12.
Kambeitz, J., Kambeitz-Ilankovic, L., Cabral, C., Dwyer, D.B., Calhoun, V.D., van den Heuvel, M.P., Falkai, P., Koutsouleris, N., Malchow, B., 2016. Aberrant functional whole-brain network architecture in patients with schizophrenia: a meta-analysis. Schizophr. Bull. 42 (Suppl. 1), S13–S21.
Kandylaki, K.D., Nagels, A., Tune, S., Wiese, R., Bornkessel-Schlesewsky, I., Kircher, T., 2015. Processing of false belief passages during natural story comprehension: an fMRI study. Hum. Brain. Mapp. 36, 4231–4246.
Klumpp, H., Keutmann, M.K., Fitzgerald, D.A., Shankman, S.A., Phan, K.L., 2014. Resting state amygdala-prefrontal connectivity predicts symptom change after cognitive behavioral therapy in generalized social anxiety disorder. Biol. Mood. Anxiety Disord. 4, 14.
Lang, S., Yu, T., Markl, A., Muller, F., Kotchoubey, B., 2011. Hearing others' pain: neural activity related to empathy. Cogn. Affect. Behav. Neurosci. 11, 386–395.
Latora, V., Marchiori, M., 2001. Efficient behavior of small-world networks. Phys. Rev. Lett. 87, 198701.
Leary, M.R., 1983. A brief version of the fear of negative evaluation scale. Pers. Soc. Psychol. Bull., 9.
Liebowitz, M.R., 1987. Social phobia. Mod. Probl. Pharm. 22, 141–173.
Liu, F., Guo, W., Fouche, J.P., Wang, Y., Wang, W., Ding, J., Zeng, L., Qiu, C., Gong, Q., Zhang, W., Chen, H., 2015a. Multivariate classification of social anxiety disorder using whole brain functional connectivity. Brain. Struct. Funct. 220, 101–115.
Liu, F., Zhu, C., Wang, Y., Guo, W., Li, M., Wang, W., Long, Z., Meng, Y., Cui, Q., Zeng, L., Gong, Q., Zhang, W., Chen, H., 2015b. Disrupted cortical hubs in functional brain networks in social anxiety disorder. Clin. Neurophysiol. 126, 1711–1716.
Luo, S., Shi, Z., Yang, X., Wang, X., Han, S., 2014. Reminders of mortality decrease midcingulate activity in response to others' suffering. Soc. Cogn. Affect. Neurosci. 9, 477–486.
Manning, J., Reynolds, G., Saygin, Z.M., Hofmann, S.G., Pollack, M., Gabrieli, J.D., Whitfield-Gabrieli, S., 2015. Altered resting-state functional connectivity of the frontal-striatal reward system in social anxiety disorder. PLoS One 10, e0125286.
Maslov, S., Sneppen, K., 2002. Specificity and stability in topology of protein networks. Science 296, 910–913.
Mattick, R.P., Clarke, J.C., 1998. Development and validation of measures of social phobia scrutiny fear and social interaction anxiety. Behav. Res. Ther. 36, 455–470.
Newman, M.E., 2006. Modularity and community structure in networks. Proc. Natl. Acad. Sci. USA 103, 8577–8582.
Ohayon, M.M., Schatzberg, A.F., 2010. Social phobia and depression: Prevalence and comorbidity. J. Psychosom. Res 68, 235–243.
Pannekoek, J.N., Veer, I.M., van Tol, M.J., van der Werff, S.J., Demenescu, L.R., Aleman, A., Veltman, D.J., Zitman, F.G., Rombouts, S.A., van der Wee, N.J., 2013. Resting-state functional connectivity abnormalities in limbic and salience networks in social anxiety disorder without comorbidity. Eur. Neuropsychopharmacol. 23, 186–195.
Park, J.Y., Kim, J.H., 2010. Korean version of the sheehan disability scale (sds): Reilability and validity. Kor. J. Clin. Psychol. 29, 73–81.
Pejic, T., Hermann, A., Vaitl, D., Stark, R., 2013. Social anxiety modulates amygdala activation during social conditioning. Soc. Cogn. Affect. Neurosci. 8, 267–276.
Peterson, A., Thome, J., Frewen, P., Lanius, R.A., 2014. Resting-state neuroimaging studies: a new way of identifying differences and similarities among the anxiety disorders? Can. J. Psychiatry 59, 294–300.
Power, J.D., Schlaggar, B.L., Lessov-Schlaggar, C.N., Petersen, S.E., 2013. Evidence for hubs in human functional brain networks. Neuron 79, 798–813.
Prater, K.E., Hosanagar, A., Klumpp, H., Angstadt, M., Phan, K.L., 2013. Aberrant amygdala-frontal cortex connectivity during perception of fearful faces and at rest in generalized social anxiety disorder. Depress. Anxiety 30, 234–241.
Qiu, C., Zhu, C., Zhang, J., Nie, X., Feng, Y., Meng, Y., Wu, R., Huang, X., Zhang, W., Gong, Q., 2014. Diffusion tensor imaging studies on chinese patients with social anxiety disorder. Biomed. Res. Int 2014, 860658.
Qiu, C.J., Feng, Y., Meng, Y.J., Liao, W., Huang, X.Q., Lui, S., Zhu, C.Y., Chen, H.F., Gong, Q.Y., Zhang, W., 2015. Analysis of altered baseline brain activity in drug-naive adult patients with social anxiety disorder using resting-state functional mri. Psychiatr. Invest. 12, 372–380.
Rosvall, M., Bergstrom, C.T., 2008. Maps of random walks on complex networks reveal community structure. Proc. Natl. Acad. Sci. USA 105, 1118–1123.
Rubinov, M., Sporns, O., 2010. Complex network measures of brain connectivity: uses and interpretations. Neuroimage 52, 1059–1069.
Shang, J., Fu, Y., Ren, Z., Zhang, T., Du, M., Gong, Q., Lui, S., Zhang, W., 2014. The common traits of the acc and pfc in anxiety disorders in the dsm-5: meta-analysis of voxel-based morphometry studies. PLoS One 9, e93432.
Sheehan, D.V., 1983. The Anxiety Disease. Charles Scribner and Sons, New York.
Shin, D.J., Jung, W.H., He, Y., Wang, J., Shim, G., Byun, M.S., Jang, J.H., Kim, S.N., Lee, T.Y., Park, H.Y., Kwon, J.S., 2014. The effects of pharmacological treatment on functional brain connectome in obsessive-compulsive disorder. Biol. Psychiatry 75, 606–614.
Stein, M.B., Goldin, P.R., Sareen, J., Zorrilla, L.T., Brown, G.G., 2002. Increased amygdala activation to angry and contemptuous faces in generalized social phobia. Arch. Gen. Psychiatry 59, 1027–1034.
Stein, M.B., Kean, Y.M., 2000. Disability and quality of life in social phobia: Epidemiologic findings. Am. J. Psychiatry 157, 1606–1613.
Stein, M.B., Stein, D.J., 2008. Social anxiety disorder. Lancet 371, 1115–1125.
Tomasi, D., Volkow, N.D., 2012. Resting functional connectivity of language networks: characterization and reproducibility. Mol. Psychiatry 17, 841–854.
Tzourio-Mazoyer, N., Landeau, B., Papathanassiou, D., Crivello, F., Etard, O., Delcroix, N., Mazoyer, B., Joliot, M., 2002. Automated anatomical labeling of activations in spm using a macroscopic anatomical parcellation of the mni mri single-subject brain. Neuroimage 15, 273–289.
Uehara, T., Yamasaki, T., Okamoto, T., Koike, T., Kan, S., Miyauchi, S., Kira, J., Tobimatsu, S., 2014. Efficiency of a "small-world" brain network depends on consciousness level: a resting-state fmri study. Cereb. Cortex 24, 1529–1539.
van den Heuvel, M.P., Sporns, O., 2013. Network hubs in the human brain. Trends Cogn. Sci. 17, 683–696.

Warren, D.E., Power, J.D., Bruss, J., Denburg, N.L., Waldron, E.J., Sun, H., Petersen, S.E., Tranel, D., 2014. Network measures predict neuropsychological outcome after brain injury. Proc. Natl. Acad. Sci. USA 111, 14247–14252.
Watts, D.J., Strogatz, S.H., 1998. Collective dynamics of 'small-world' networks. Nature 393, 440–442.
Whitfield-Gabrieli, S., Ghosh, S.S., Nieto-Castanon, A., Saygin, Z., Doehrmann, O., Chai, X.J., Reynolds, G.O., Hofmann, S.G., Pollack, M.H., Gabrieli, J.D., 2015. Brain connectomics predict response to treatment in social anxiety disorder. Mol. Psychiatry. http://dx.doi.org/10.1038/mp.2015.109.
Xia, M., Wang, J., He, Y., 2013. Brainnet viewer: a network visualization tool for human brain connectomics. PLoS One 8, e68910.
Yoon, H.J., Kim, J.S., Shin, Y.B., Choi, S.H., Lee, S.K., Kim, J.J., 2016. Neural activity during self-referential working memory and the underlying role of the amygdala in social anxiety disorder. Neurosci. Lett. 627, 139–147.
Yu, T., Lang, S., Birbaumer, N., Kotchoubey, B., 2011. Listening to factually incorrect sentences activates classical language areas and thalamus. Neuroreport 22, 865–869.